ISSN 1983-1838

(DOI): 10.18624/etech.v17i1.1322

PRODUCTIVITY GAIN IN WIRE ARC ADDITIVE MANUFACTURING BROUGHT BY ROBOT-INTEGRATED COOLING SYSTEM USING COMPRESSED AIR

GANHO DE PRODUTIVIDADE OBTIDO COM SISTEMA DE RESFRIAMENTO POR AR COMPRIMIDO INTEGRADO A ROBÔ EM MANUFATURA ADITIVA POR ARCO VOLTAICO COM ARAME PROTEGIDO POR GÁS

ERWIN TEICHMANN
https://orcid.org/0000-0003-0951-9151/ erwin@ifsc.edu.br
Instituto Federal de Educação, Ciência e Tecnologia de Santa Catarina - IFSC – Florianópolis, Santa Catarina

LUCIANO AMAURY DOS SANTOS
https://orcid.org/0009-0003-1691-3891/ luciano.santos@ifsc.edu.br
Instituto Federal de Educação, Ciência e Tecnologia de Santa Catarina - IFSC – Florianópolis, Santa Catarina

FELIPE TABATA FUKUSHIMA
https://orcid.org/0009-0005-4212-9368/ felipefuku2000@gmail.com
Instituto Federal de Educação, Ciência e Tecnologia de Santa Catarina - IFSC – Florianópolis, Santa Catarina

GUILLEN ETCHEMENDY
https://orcid.org/0009-0000-0573-7501/ guillen.etchemendy@viacesi.fr
CESI École d'Ingénieurs, França.

TEO BOUTILLIER
https://orcid.org/0009-0006-7782-6785/ teo.boutillier@viacesi.fr
CESI École d'Ingénieurs, França.

RAFAEL NUNES
https://orcid.org/0000-0003-4208-679X / rafael.Nunes@bil-ibs.be
Belgisch Instituut voor Lastechniek Bélgica.

Recebido em: 22/02/2024.
Aprovado em: 09/09/2024.
Publicado em: 24/09/2024.

ISSN 1983-1838

(DOI): 10.18624/etech.v17i1.1322

PRODUCTIVITY GAIN IN WIRE ARC ADDITIVE MANUFACTURING BROUGHT BY ROBOT-INTEGRATED COOLING SYSTEM USING COMPRESSED AIR

ERWIN TEICHMANN
LUCIANO AMAURY DOS SANTOS
FELIPE TABATA FUKUSHIMA
GUILLEN ETCHEMENDY
TEO BOUTILLIER
RAFAEL NUNES

ABSTRACT

The international ISO/ASTM 52900 terminology classifies Wire Arc Additive Manufacturing (WAAM) as part of the group of Directed Energy Deposition (DED) of Additive Manufacturing (AM) processes for metallic pieces. These processes involve heat accumulation in some areas of a workpiece, which can possibly lead to thermal deformations, an excessively large weld pool and geometric defects. To avoid this, a common practice is the use of dwell times, where one stops the metal deposition and waits for the piece to cool down to a pre-determined temperature before resuming it, causing the productivity to plummet. The work presented in this paper studies a robot-integrated cooling system for WAAM applying compressed air, that shortens the dwell time needed to achieve a good quality piece using affordable and light equipment. Its goal is to assess the productivity gain attainable in the fabrication of a small (45 mm in height × nearly 50 mm in diameter) hollow piece of low carbon steel by WAAM using the forementioned cooling system. Experiments were performed and a simple mathematical model (avoiding the costs of Finite Elements models) to the essential heat transfer phenomena involved in the problem was put together and tested. The mathematical model overestimated the shortening of the cooling time, but the experiments confirmed the expected productivity gain, with the cooling system using compressed air allowing a 60 % reduction in the time needed to build a piece within acceptable geometrical tolerance limits.

]**Keywords:** Compressed-air cooling; Mathematical modeling; WAAM cooling; WAAM productivity.

ABSTRACT

A terminologia internacional da ISO/ASTM 52900 coloca a manufatura aditiva por arco voltaico com arame (WAAM) dentro do grupo dos processos de manufatura aditiva por Deposição de Energia Direcionada (DED) para peças metálicas. Estes processos envolvem o acúmulo de calor em algumas áreas da peça, podendo causar deformações térmicas, uma poça de fusão excessivamente grande e defeitos geométricos. Para evitar isso, uma prática comum é a utilização de tempos de parada, onde se interrompe a deposição do metal e se espera que a peça esfrie até uma temperatura pré-determinada antes de retomá-la, fazendo com que a produtividade despenque. O trabalho apresentado neste artigo estuda um sistema de resfriamento integrado ao robô para WAAM aplicando ar comprimido, que reduz o tempo de parada necessário para obter uma peça de boa qualidade usando equipamento leve e acessível. O objetivo é avaliar o ganho de produtividade atingível na fabricação de uma pequena peça oca (45 mm de altura x quase 50 mm de diâmetro) de aço baixo carbono pela WAAM utilizando o sistema de refrigeração mencionado. Experimentos foram realizados e um modelo matemático simples (evitando os custos dos modelos de Elementos Finitos) para os fenômenos essenciais de transferência de calor envolvidos no problema foi montado e testado. O modelo matemático superestimou a redução do tempo de resfriamento, mas os experimentos confirmaram o ganho de produtividade esperado, com o resfriamento por ar comprimido, permitindo uma redução de 60% no tempo necessário para a construção de uma peça dentro de limites de tolerância geométrica aceitáveis.

Palavras-chave: Modelamento matemático; Produtividade no processo WAAM; Resfriamento por ar comprimido; Resfriamento no processo WAAM.

ISSN 1983-1838

(DOI): 10.18624/etech.v17i1.1322

PRODUCTIVITY GAIN IN WIRE ARC ADDITIVE MANUFACTURING BROUGHT BY ROBOT-INTEGRATED COOLING SYSTEM USING COMPRESSED AIR

ERWIN TEICHMANN
LUCIANO AMAURY DOS SANTOS
FELIPE TABATA FUKUSHIMA
GUILLEN ETCHEMENDY
TEO BOUTILLIER
RAFAEL NUNES

1 INTRODUCTION

The method of Additive Manufacturing (AM) consists of layer-by-layer material deposition, gradually accumulating material in such a manner that, eventually, results in a three-dimensional object (LE *et al*., 2021). The terminology presented by ISO (2021) groups many processes with the widely denominated Wire Arc Additive Manufacturing (WAAM) under the label of Directed Energy Deposition (DED) processes, without standardizing the detailing of how the energy and metal deposition happen. So, recurring to welding terminology (ISO, 2016), it is convenient to mention that the present study is focused on the Metal Active Gas (MAG) based process. The American Welding Society (AWS, 2023) suggests a more compact description: Gas Metal Arc Directed Energy Deposition (GMA-DED) process.

However, heating metals by electric arc brings a challenge due to its inherent nature: intense heat accumulation (WU *et al*., 2017). As layers are made, metal tends to retain heat for extended periods, becoming a critical factor. Elevated temperatures between layer depositions cause delayed solidification of the melt pool, resulting in parts with reduced height and increased width. In such situations the need of periodic deposition interruption by a dwell time (while the piece cools down) comes about.

The necessary time itself to achieve the desired dwell temperature is not constant, since the first layers have normally higher temperature gradient and heat dissipation due to the proximity of the substrate. Besides the evident and above mentioned financial and productivity disadvantages caused by that, the deformation induced by the aggressive WAAM thermal cycles brings a very significant complexity in the machining posterior to the WAAM process (NUNES *et al*., 2023).

The cooling system (TEICHMANN *et al*., 2019) discussed in the present work was developed to alleviate these problems caused by accumulated heat. The hardware it adds to the basic WAAM equipment is quite simple. It is built by attaching to the weld torch a metal outlet for a 4 mm pneumatic line controlled through a solenoid valve by the robot.

ISSN 1983-1838

(DOI): 10.18624/etech.v17i1.1322

ERWIN TEICHMANN
LUCIANO AMAURY DOS SANTOS
FELIPE TABATA FUKUSHIMA
GUILLEN ETCHEMENDY
TEO BOUTILLIER
RAFAEL NUNES

A primary objective of this work, besides the investigation of productivity, was to demonstrate that specialized and expensive machinery and instruments are not required to perform WAAM, addressing a common concern among companies that claim otherwise. For this purpose, buying parts dedicated exclusively to WAAM cooling was avoided. All equipment used was already available at the laboratory where the system was assembled, and the parts can be replaced by similar ones.

2 EQUIPMENT AND MATERIAL

Although additive manufacturing and WAAM process itself has been attracting attention from all industrial sectors, there is still a misleading concept that complex and expensive equipment to perform and fabricate 3D components is requisite. This concept concerns to hardware, software, and materials as well, which is not completely valid for simple structures and components (NUNES *et al*., 2023).

The workplace setup, as shown in Figure 1, was comprised of:

- Merkle High Pulse 350K Generator: The central machine of the process, offers advanced arc control and welding parameter management capabilities;
- IMC UPR-7500 Liquid Cooler: This device was used to dissipate the heat generated within the welding torch;
- FANUC robot, M-10iA model: 6 axis robot used to move the welding torch to produce the workpiece (it can be replaced by any system containing at least 3 degree of freedom);
- FANUC controller, 30i model, and its Teach Pendant (a device connected to the computer, containing a screen that allows the user to view programs): The controller for the robot, in which all programs were made and executed, including the movement commands, compressed air output management as well as the weld feeder activation;
- 82% Argonium and 18% Oxygen as shielding gas;
- Copper covered steel wire ER76S-6, 1.0 mm diameter;

ISSN 1983-1838

(DOI): 10.18624/etech.v17i1.1322

- A steel tube, 3.65 mm internal diameter, was used as compressed air outlet;
- Digital Infrared Thermometer;
- Fluke VT04A Visual IR Thermometer;
- Instrutemp Pressure and Flow Meter.

Figure 1 – Experimental setup: on the left (a) a general view and on the right (b) a close view of the cooling compressed air outlet attached to the welding torch by a 3D printed polymeric clamp

(a) 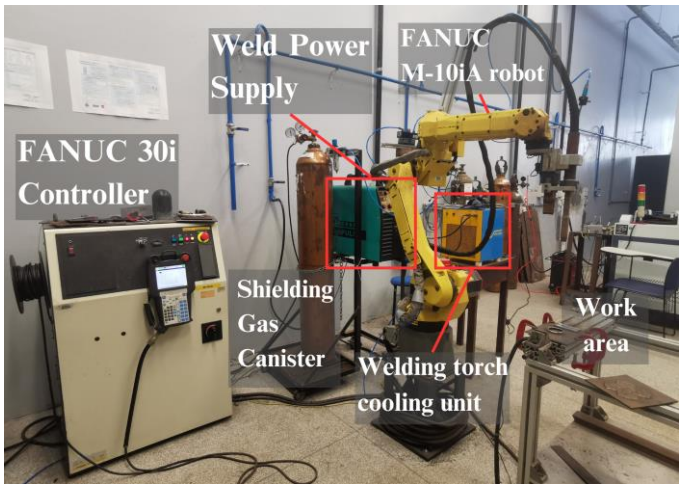

(b) 

Source: Fukushima (2023)

Both thermometers were used for temperature monitoring, and the Flow Meter, to measure the compressed air speed.

The welding parameters used on the Merkle power supply were as follows:

ISSN 1983-1838

(DOI): 10.18624/etech.v17i1.1322

Table 1 – Welding parameters

Parameter	Value	Unit
Throat (weld penetration depth)	1.5	-
Process	Cold	-
Stitch/inter	OFF	-
Pre-gas time	0.2	s
Start time	0	s
Downslope	0	s
Post-weld Gas flow	0.2	s
Burnback rate	30%	-
Choke	0%	-
Current	70	A
Voltage	15.4	V
Robot movement speed during welding	30	cm/min

Source: Fukushima (2023)

3 STEPS TO ROBOT PROGRAMMING

3.1 Defining the Workpiece Geometry.

The test piece shape was inspired by the one used by Kozamernik *et al*. (2020), that also studied a WAAM cooling system, albeit through a different cooling method. That nearly hyperboloidal shape was decided upon because of its positive and negative angles of 50°, allowing for an evaluation of tilted walls production.

The initial design was created using SolidWorks, as shown in Figure 2, and later imported into Fusion 360, where horizontal geometrical planes were generated, manually slicing the workpiece. Four distributed points were defined at each layer, and the coordinates for each were

ISSN 1983-1838

(DOI): 10.18624/etech.v17i1.1322

registered to generate circular movements afterwards. The basic piece dimensions are presented in Table 2.

Figure 2 – Workpiece 3D CAD model

Source: Fukushima (2023)

Table 2 – Basic piece dimensions

Dimension	Value	Unit
Maximum External Diameter	62.5	mm
Minimum External Diameter	42.5	mm
Thickness	4	mm
Height	45	mm

Source: Fukushima (2023)

For each layer, the linear and circular movement commands were manually set, entering the coordinate values for each point, with the starting point of each level being displaced 45° clockwise, according to the deposition strategy that will be further explained in the next section.

ISSN 1983-1838

(DOI): 10.18624/etech.v17i1.1322

ERWIN TEICHMANN
LUCIANO AMAURY DOS SANTOS
FELIPE TABATA FUKUSHIMA
GUILLEN ETCHEMENDY
TEO BOUTILLIER
RAFAEL NUNES

3.2 Deposition Strategy.

The production strategy applied was to execute two layers, and subsequently apply either a dwell time or forced cooling, with the purpose of lowering the temperature to 100 °C, avoiding energy accumulation throughout the process. The threshold temperature was defined according to prior tests, in which was observed what temperature would be best to prevent overheating.

In line with Verlinde *et al*. (2021), the deposition strategy must take the heat generation into account. Figure 3(a) exemplifies a piece made without varying the layer's start/end point, leading to heat accumulation and uneven height. Therefore, to avoid this phenomenon, the recommendation for closed contours is to shift each tier's start/end point, as shown in Figure 3(b). In this project, the start/end point was rotated 45° at each level and after the end of each layer deposition, the torch was raised by 1.6 mm.

Figure 3 – Start/end points: (a) in the same position for every layer and (b) displaced by 45º in successive layers

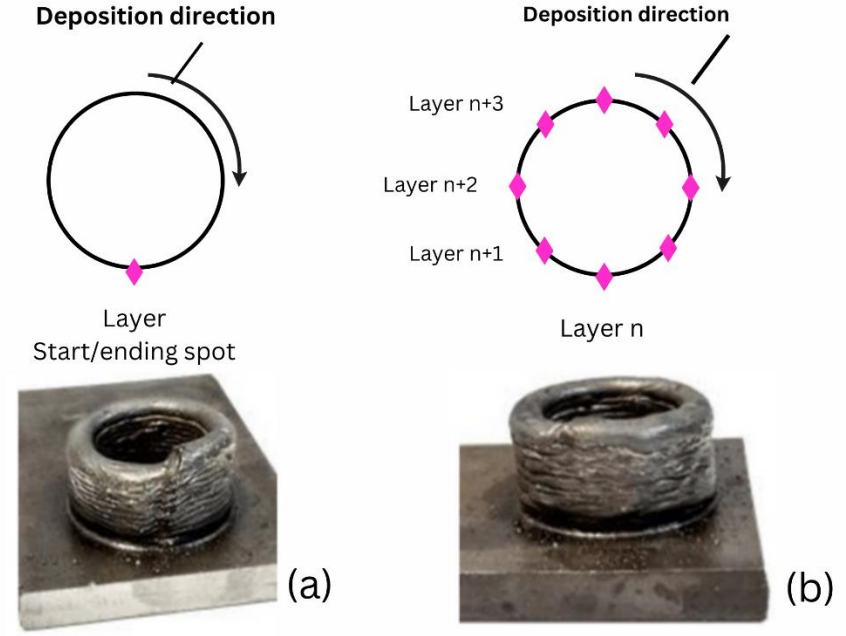

Source: Adapted from Verlinde *et al*. (2021)

ISSN 1983-1838

(DOI): 10.18624/etech.v17i1.1322

ERWIN TEICHMANN
LUCIANO AMAURY DOS SANTOS
FELIPE TABATA FUKUSHIMA
GUILLEN ETCHEMENDY
TEO BOUTILLIER
RAFAEL NUNES

3.3 Anthropomorphic Robot Programming.

A thriving trend in WAAM development is the streamlined tool (welding torch or compressed air outlet) path generation based on the piece's CAD model, resulting in the program code needed to control the movements of the torch and/or the piece being manufactured (FERREIRA, 2022; MX3D, 2024; SPRUTCAM, 2024). It was not available to the authors, however, a software compatible with the FANUC M-10iA robot to perform this task. For this reason, extensive manual robot programming was needed.

To program the robot, it was necessary to analyze the 3D model. For each layer, five points had to be specified: the first, being an approach point, to which the robot moves linearly in higher speed; the activation of the welding power supply by toggling a Digital Output; followed by circular arc movements to the other four points with a speed of 30 cm/min (that provided adequate metal deposition in preliminary tests).

An obstacle was encountered during the development of the compressed air passage movements, because the piece consists of circles of varied diameters, meaning that the most recent layer would have a differing circumference from the one before it. The simpler solution employed makes use of Position Registers (PR), a feature available in FANUC's system that allows the user to store points' coordinate values in PR variables, so that they can be calculated without impacting the original program.

4 HEAT TRANSFER MATHEMATICAL MODEL

4.1 Heat Conduction in an Infinite Cylindrical Tube.

To better understand the effects of variables such as piece wall thickness and perimeter, its material thermophysical properties, heat source power, heat source velocity and heat transfer

ISSN 1983-1838

(DOI): 10.18624/etech.v17i1.1322

ERWIN TEICHMANN
LUCIANO AMAURY DOS SANTOS
FELIPE TABATA FUKUSHIMA
GUILLEN ETCHEMENDY
TEO BOUTILLIER
RAFAEL NUNES

coefficient at piece's surfaces over the cooling time (dwell time) between deposition cycles, a model like the one presented by Santos and Silva (2002) following Rosenthal (1941) is useful. This model is expressed by equations (1) and (2), in which the variables presented in Table 3 are used.

$$T(\theta,z,t)-T_0 = \int_{t_0}^{\min(t_1,t)} \frac{q}{\pi k R W}\sqrt{\frac{\alpha}{4\pi(t-\tau)}}\, e^{\left[-\frac{\alpha h_1 (t-\tau)}{kW}-\frac{z^2}{4\alpha(t-\tau)}\right]} \times\left\{\frac{1}{2}+\sum_{n=1}^{\infty} e^{\left[-\alpha\left(\frac{n}{R}\right)^2(t-\tau)\right]}\cos[n(\theta-\Omega\tau)]\right\}\mathrm{d}\tau \quad \text{if} \quad t\le t_2 \qquad (1)$$

$$T(\theta,z,t)-T_0 = e^{\left[-\frac{\alpha h_2 (t-t_2)}{kW}\right]}\int_{t_0}^{t_1} \frac{q}{\pi k R W}\sqrt{\frac{\alpha}{4\pi(t-\tau)}}\, e^{\left[-\frac{\alpha h_1 (t_2-\tau)}{kW}-\frac{z^2}{4\alpha(t-\tau)}\right]} \times\left\{\frac{1}{2}+\sum_{n=1}^{\infty} e^{\left[-\alpha\left(\frac{n}{R}\right)^2(t-\tau)\right]}\cos[n(\theta-\Omega\tau)]\right\}\mathrm{d}\tau \quad \text{if} \quad t> t_2 \qquad (2)$$

Table 3 – Variables used in the temperature field expressions (1) and (2)

Symbol	Quantity	Unit	Value
T	piece temperature	ºC	many
T_0	initial temperature	ºC	25
θ	azimuthal coordinate	rad	many
z	vertical coordinate	m	many
t	time	s	many
q	heat source power	W	1624
t_0	heat source turn on instant	s	0
t_1	heat source turn off instant	s	62.8
t_2	forced cooling start instant	s	64.8 or ∞
k	thermal conductivity	W/(m.K)	40
α	thermal diffusivity	m²/s	8×10^{-6}

ISSN 1983-1838

(DOI): 10.18624/etech.v17i1.1322

PRODUCTIVITY GAIN IN WIRE ARC ADDITIVE MANUFACTURING BROUGHT BY ROBOT-INTEGRATED COOLING SYSTEM USING COMPRESSED AIR

ERWIN TEICHMANN
LUCIANO AMAURY DOS SANTOS
FELIPE TABATA FUKUSHIMA
GUILLEN ETCHEMENDY
TEO BOUTILLIER
RAFAEL NUNES

R	cylinder radius	m	0.025
W	cylinder wall thickness	s	0.005
τ	dummy variable	s	many
h_1	natural convection heat transfer coefficient	W/(m².K)	45
h_2	forced convection heat transfer coefficient	W/(m².K)	166 or 205
Ω	heat source rotational speed	rad/s	0.2

Source: Fukushima (2023)

The values shown in Table 3 were chosen to represent the WAAM process using low carbon steel wire and the heat source power was obtained by multiplying values of current and voltage usually found, multiplied by a thermal efficiency of 0.8 (this value and those of thermal properties are found in books like that of Grong (1997)) and also multiplied by a factor 2, since the temperature field expressions were derived for an infinite cylindrical tube (but the main interest is only the half domain below the horizontal symmetry plane).

The heat transfer coefficients h_1 and h_2 represent not only convection but also contain an estimate of some heat loss by radiation, particularly relevant in the case of natural convection. The convection contribution was obtained by using correlations collected in the book of Bergman *et al*. (2011), but in the case of forced convection (by an impinging jet) the velocity at the jet's origin must be known. The next subsection deals with how to obtain this velocity value knowing the pressure setting at the compressed air regulator that is part of the experimental apparatus.

Figure 4(a) depicts the temperature field described by (1) at $t = t_1$. Figure 4(b) shows temperature cycles predicted using (1) and (2) at a point 15 mm distant from the heat source trajectory for three different conditions: natural convection from start to end ($t_2 = \infty$); forced convection starting at t_2 = 64.8 s with the compressed air regulator set at 4 bar (h_2 = 166 W/(m².K));

ISSN 1983-1838

(DOI): 10.18624/etech.v17i1.1322

forced convection starting at t_2 = 64.8 s with the compressed air regulator set at 6 bar (h_2 = 205 W/(m².K)).

Figure 4 – Theoretical results: (a) temperature field at the end of two (clockwise, seen from above) turns of the heat source and (b) temperature cycles at a point 15 mm below the upper plane

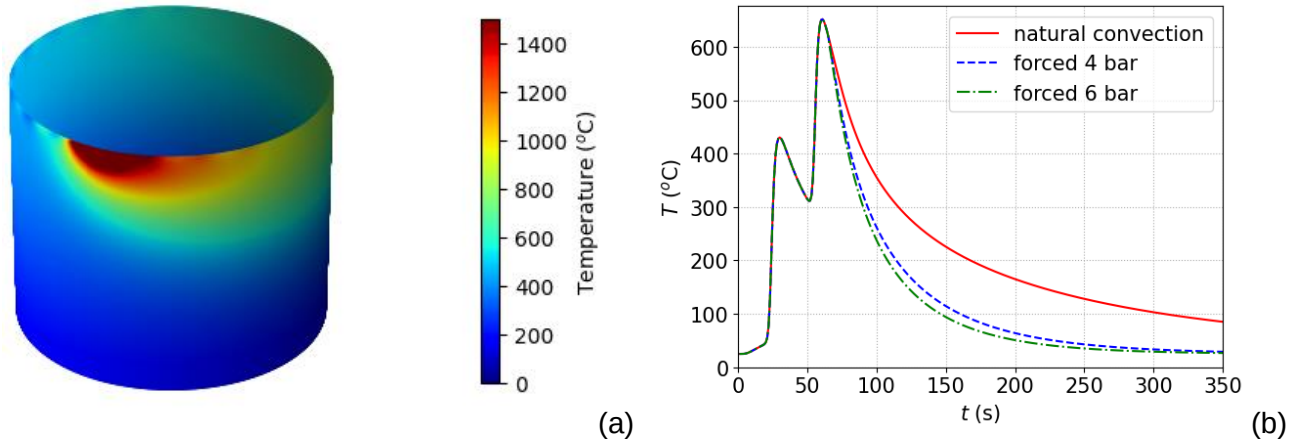

(a) (b)

Source: Fukushima (2023)

4.2 Air Speed Estimation.

The relation between the air velocity at the tube outlet and the pressure set in an air regulator upstream is not very simple due to the possibility of choked flow occurrence. The choked flow, that is insensitive to variations in pressure downstream of a throat, frequently occurs when compressed air is discharged to atmosphere.

From the air regulator to the air outlet in the experimental apparatus there are 385 cm of nylon tube with 4 mm internal diameter and 22,4 cm of a steel tube with 3.65 mm internal diameter, besides the robot-integrated solenoid valve. In the relatively long nylon tube and the valve, the friction (without significant temperature variation) is the main cause of persistent air expansion. The

ISSN 1983-1838

(DOI): 10.18624/etech.v17i1.1322

isothermal compressible flow model available at Bar-Meir (2007) and Shapiro (1953) describes reasonably this part of the pneumatic circuit.

The 8.75 % area reduction when the air enters the steel pipe almost at the air outlet cannot be disregarded, and so the isothermal flow model was combined with the isentropic model presented in standard fluid mechanics textbooks (ÇENGEL; CIMBALA, 2015). This leads to a nonlinear system of three equations

$$\begin{cases} f\dfrac{L}{D} = \ln\left(\dfrac{M_1^2}{M_2^2}\right) + \dfrac{1}{\gamma}\left(\dfrac{1}{M_1^2} - \dfrac{1}{M_2^2}\right) \\ \dfrac{d^2}{D^2} = \dfrac{M_2}{M_3}\left[\dfrac{2+(\gamma-1)M_3^2}{2+(\gamma-1)M_2^2}\right]^{\frac{\gamma+1}{2(\gamma-1)}} \\ \dfrac{p_3}{p_1} = \dfrac{M_1}{M_2}\left[\dfrac{2+(\gamma-1)M_2^2}{2+(\gamma-1)M_3^2}\right]^{\frac{\gamma}{\gamma-1}} \end{cases} \tag{3}$$

where the Mach numbers M_1, M_2 and M_3 are the unknown. It is assumed that the pressures p_1, at the regulator, and p_3, at the steel tube outlet are known, as are the diameter of the nylon tube, D, and that of the steel tube, d, the specific heat ratio γ (1.4 for air), and the nylon tube equivalent length L. The friction factor f is calculated using an appropriate correlation (ÇENGEL; CIMBALA, 2015). Due to the difficulty in estimating the local head losses at the air regulator and the solenoid valve, L was adjusted using velocity measurements taken at the jet produced at the air outlet. This adjustment is the subject of the next subsection.

Another apparent difficulty is that the indicated pressure at the compressed air regulator is closer to the total pressure than to the static pressure appearing in the formulation above. Nonetheless, it is not an issue, as the relation between static pressure p and total pressure p_t in a perfect gas flow is simply $p_t = p\,(1 + M^2\gamma/2)$.

The temperature within the nylon tube is considered equal to ambient temperature. But as the compressed air flows from the nylon tube to the steel tube, the air temperature is lowered to

ISSN 1983-1838

(DOI): 10.18624/etech.v17i1.1322

ERWIN TEICHMANN
LUCIANO AMAURY DOS SANTOS
FELIPE TABATA FUKUSHIMA
GUILLEN ETCHEMENDY
TEO BOUTILLIER
RAFAEL NUNES

$$T_{\text{outlet}} = \left[\frac{2+(\gamma-1)M_2^2}{2+(\gamma-1)M_3^2}\right] T_\infty \tag{4}$$

The velocity at the outlet is then obtained using

$$V_{\text{outlet}} = M_3\sqrt{\gamma R T_{\text{outlet}}} \tag{5}$$

where R is the perfect gas constant of the fluid (287 J/(kg.K) for air).

4.3 Compressed air tube equivalent length adjustment.

As the velocity at the compressed air outlet is hard to measure, velocities at the jet origin were taken using a Pitot-static probe, and then the outlet velocity was inferred using a model describing the whole air jet. A summarized presentation of this model for a round jet, that is more thoroughly discussed by Pope (2000) can be found in Cushman-Roisin (2022) and it leads to the equation

$$V_{\text{jet}}(x,r) = V_{\text{outlet}} \frac{d}{x+x_b}\sqrt{\frac{b}{2}}\, e^{\left[-b\left(\frac{r}{x+x_b}\right)^2\right]} \tag{6}$$

where x is the coordinate parallel to the jet symmetry axis, with the origin ($x = 0$) at the compressed air outlet and r (the radial coordinate) perpendicular to x (the origin $r = 0$ coinciding with the jet symmetry axis), d is the compressed air outlet diameter, b and x_b are parameters of the model. Cushman-Roisin (2022) gives the values $I = 50$ and $x_b = 2\,d/5$, but the measurements made in the present work revealed a narrower jet, with $b = 79$ and $x_b = 0.78\,d$ (taking $d = 3.65$ mm).

With this model for the air jet, and measured velocities along the jet, the velocity at the compressed air outlet can be estimated. With the compressed air regulator set at 6 bar this velocity estimate was about the speed of sound (340 m/s). With the regulator set at 4 bar, around 245 m/s. Using these velocity estimates the nylon tube equivalent length was estimated to be $L = 7.3$ m (much larger than the true length, as expected).

ISSN 1983-1838

(DOI): 10.18624/etech.v17i1.1322

5 WAAM EXPERIMENTAL RESULTS

5.1 Tests.

A total of four experimental trials were carried out, with different purposes. Table 4 shows the main parameters: compressed air pressure and dwell time, when used.

Table 4 – Test parameters

Test number	Air Pressure bar	Dwell Time seconds	Total Production Time minutes
1	-	-	16
2	-	240	105
3	4	100	42
4	6	100	42

Source: Fukushima (2023)

Test 1 was conducted to observe the effect of ignoring the heat accumulation by not using dwell time and any forced cooling technique, while tests 2 and 3 were performed to assess the potential productivity gain brought using compressed air to cool the piece. Test 4 was to verify the effect of an increase in the compressed air regulator pressure.

The term “dwell time” in this context, found in the literature (WU *et al*., 2017) and sometimes replaced by interpass time, holding time or idle time (LE *et al*., 2021), means the duration of an interruption in the metal deposition while the piece cools down (with or without the help of a compressed air jet).

In the preparatory trials before the experiments reported previously, an average temperature of 100 ºC was selected as a threshold for the piece cooling after two layers of metal deposition: when reached after each dwell time, the resulting geometry of the obtained piece was deemed acceptable. The following step, still in those trials, was the search of the minimum dwell times needed to reach

ISSN 1983-1838

(DOI): 10.18624/etech.v17i1.1322

this threshold with and without cooling by compressed air. The dwell times found are those reported in Table 4.

Comparing abscissa values in Figure 4(b) with dwell times in Table 4, one can observe that the cooling (either by natural convection or by compressed air) was reasonably described by the mathematical model (that, to reach 100 ºC, predicted around 240 s of cooling time by natural convection and 100 s with forced convection by the compressed air jet). Considering that the correlation for heat transfer by impinging jets available at of Bergman *et al*. (2011) was not developed for the piece geometries discussed here (but for heat transfer between the jet and a flat surface perpendicular to it, not for a nearly cylindrical geometry with walls parallel to the jet) its prediction ability seems pretty satisfactory. An interesting aspect in adapting that correlation was the choice of some values it requires. The first choice to be made was that of the distance between the jet origin and the piece (the results here presented were obtained by using the 25 mm kept between the compressed air outlet and the top of the piece, but an alternative could be to use the 70 mm kept between that outlet and the base plate at the piece conclusion (this was attempted and did not significantly change the results). The second and more important choice was how to compute the ratio of the jet outlet area to the cooled surface area. Both faces of the nearly cylindrical piece plus both faces of the base plate were used in the calculation of the cooled surface area to obtain the theoretical results shown in Figure 4.

Test number 1, although the quickest, had the purpose be a reference on the low quality the piece would have if no dwell times nor compressed air were applied. Test number 2 applied the common technique of dwell times at each two layers, resulting in a taller piece. At test number 3, instead of just employing deposition interruptions, a jet of compressed air at 4 bar was applied to the piece surface during the dwell times at each two layers. At test 4 the compressed air was regulated at 6 bar. The geometric errors were evaluated via laser scanning and measuring with a precision caliper. The results of this evaluation are presented in the following subsection. A significant 60 % increase in productivity is obtained comparing the Total Production time of pieces 2 and 3 shown in Table 4.

ISSN 1983-1838

(DOI): 10.18624/etech.v17i1.1322

The 60 % productivity gain claimed here may seem exaggerated, when one finds in Kozamernik *et al*. (2020) a natural convection cooling time just 30 % larger than the forced convection one (this amounts to mere 23 % of productivity gain). What should not be overlooked in such comparison is that the small productivity gain reported by Kozamernik *et al*. (2020) befell in a configuration in which the base plate was also cooled by water circulation (their baseline was not cooling just by air natural convection, like here, but a more powerful and more difficult to assemble water cooling through baseplate system).

5.2 Test Pieces 3D Scanning.

To scan the pieces, a Hexagon articulated laser measuring arm was used, together with the Polyworks software, that allows the user to compare the scanned piece to the original 3D model evaluating the difference between the surfaces. The Figure 5 show a color scheme, where:

- warmer colors indicate a distance from the revolution axis to the piece's surface that is greater than that prescribed in the 3D model to that area;
- green indicates that that the piece and 3D model surfaces are coinciding in that area;
- colder colors indicate a distance from the revolution axis to the piece's surface that is smaller than that prescribed in the 3D model to that area.

Figure 5 – 3D scanning results: (a) Piece 1 (no dwell time, no compressed air), (b) Piece 2 (dwell time of 4 minutes, no compressed air), (c) Piece 3 (dwell time of 100 s, compressed air at 4 bar) and (d) Piece 4 (dwell time of 100 s, compressed air at 6 bar)

ISSN 1983-1838

(DOI): 10.18624/etech.v17i1.1322

eTECH
TECNOLOGIAS PARA
COMPETITIVIDADE INDUSTRIAL

PRODUCTIVITY GAIN IN WIRE ARC ADDITIVE MANUFACTURING BROUGHT BY ROBOT-INTEGRATED COOLING SYSTEM USING COMPRESSED AIR

ERWIN TEICHMANN
LUCIANO AMAURY DOS SANTOS
FELIPE TABATA FUKUSHIMA
GUILLEN ETCHEMENDY
TEO BOUTILLIER
RAFAEL NUNES

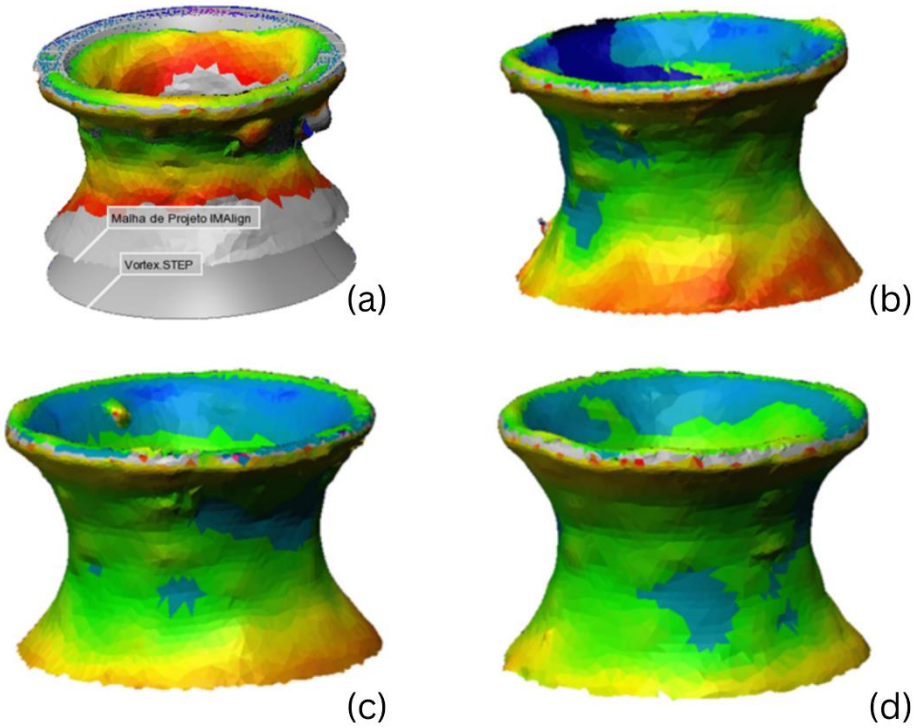

Source: Fukushima (2023)

It is possible to observe in the graph (a) of Figure 5 that there was a large height difference between the piece 1 and the original model, as well as significative geometric deviation in the radial/width direction. The graph (b) of the same figure, shows that the piece 2 quality is much better than that of piece 1, but there is still accumulated material at the bottom of the workpiece. In the graph (c) piece 3 presents a slight enhancement in this lower area, with less red areas than that of the piece 2. The overall shape seems to be smoother also. In graph (d), piece 4 shows fewer warm colors at the bottom, as well as the predominance of the green color around the piece, indicating that its shape resembles more closely that of the 3D model than the other three pieces.

ISSN 1983-1838

(DOI): 10.18624/etech.v17i1.1322

The Polyworks software also allows the user to set levels on the piece and calculate the deviation between the actual piece profile and the circular one of the original CAD model at that level (a circularity error). After averaging the absolute values of these deviations, it is possible to compare the geometrical accuracy obtained with each of the methods applied. The levels were set at each 1 mm along the piece axis of symmetry. The results are shown in Table 5 and Figure 6 shows the manufactured pieces cut in half.

Table 5 – Geometric errors

Piece number	**Height deviation mm**	**Averaged radius absolute deviation mm**
1	-12.52	1.278
2	0.30	1.056
3	-1.48	1.069
4	-1.38	0.904

Source: Fukushima (2023)

Figure 6 – Manufactured pieces where (a) used no dwell times nor compressed air; (b) used 4 minutes dwell times; (c) used compressed air at 4 bar pressure; (d) used compressed air at 6 bar pressure

ISSN 1983-1838

(DOI): 10.18624/etech.v17i1.1322

PRODUCTIVITY GAIN IN WIRE ARC ADDITIVE MANUFACTURING BROUGHT BY ROBOT-INTEGRATED COOLING SYSTEM USING COMPRESSED AIR

ERWIN TEICHMANN
LUCIANO AMAURY DOS SANTOS
FELIPE TABATA FUKUSHIMA
GUILLEN ETCHEMENDY
TEO BOUTILLIER
RAFAEL NUNES

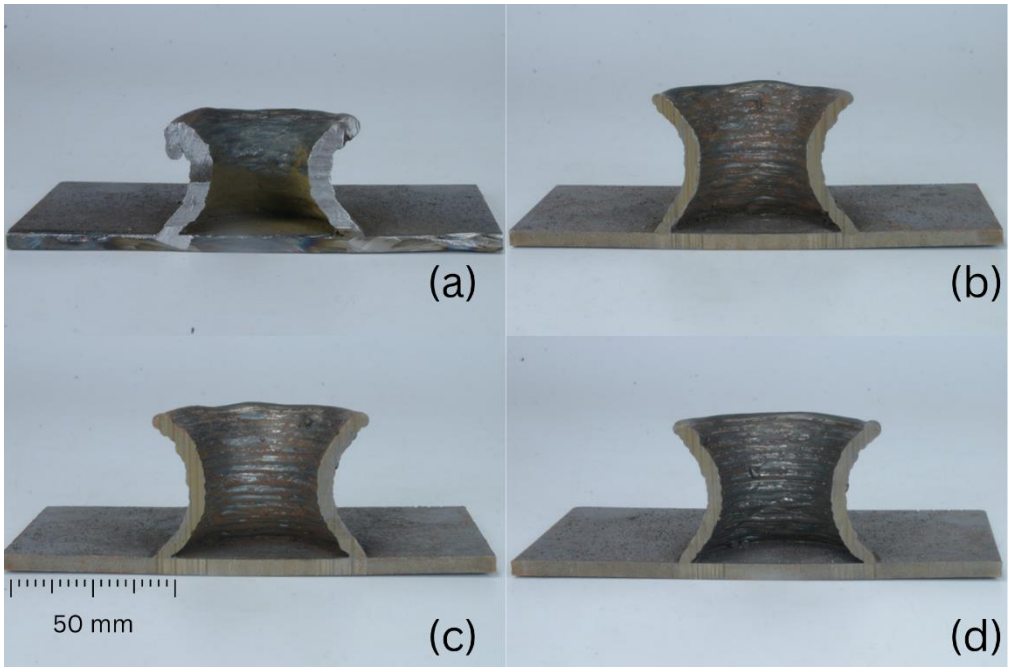

Source: Fukushima (2023)

6 CONCLUSIONS

On the matter of productivity, there was a 60% improvement, reducing the production time of 1 hour 45 minutes down to 42 minutes, proving that the use of compressed air in WAAM is indeed effective for pieces with the characteristics of those studied here.

Comparing heights, the piece 2 produced only using dwell time was higher than the piece 3 produced using 4 bar compressed air by 1.78mm (4 % of the 45 mm piece nominal height). This is probably due to the fact that the dwell time is easier to adjust when it is longer. In the last layers deposition, the 100 s of cooling by compressed air jet probably left the piece 3 warmer than piece 2 was after 240 s of natural convection cooling. The average piece temperature measurement

ISSN 1983-1838

(DOI): 10.18624/etech.v17i1.1322

procedure using low-cost infrared thermometers was not sufficiently developed or accurate to resolve this, however.

About geometric errors in the radial direction, the comparison between the pieces 3 and 4 (obtained with the same dwell time but cooled with air at different pressures) reveals some improvement obtained cooling with the higher-pressure air jet. Visually, the layers can be more clearly distinguished, and the scanning of the parts showed that the piece 4 (obtained using 6 bar) had an average radius absolute deviation 15 % lower than that of the piece 3 (obtained using 4 bar).

The heat transfer mathematical model presented here is based on a largely simplified geometry and disregards many physical phenomena present in the WAAM process. It is not expected to yield accurate estimates of the cooling time reduction provided by the compressed air jet application, but reproduced the major trends observed in the thermal aspects of the experiments. It may be helpful in the development of WAAM procedures for pieces with geometries resembling that of a cylinder. The compressed air velocity calculation procedure may also be used in heat transfer models for other geometries.

7 AKNOWLEDGMENTS

The help of many colleagues at IFSC is acknowledged, especially that of Prof. André R. de Sousa, in 3D scanning, of Prof. Marcelo Vandresen, who lent the air velocity measurement system, of Mr. Charles N. da Silva in sectioning the test pieces and of Prof. Deise A. G. Tomelin, in photographing them.

REFERENCES

AWS. **D20.1/D20.1M:2019 Specification for Fabrication of Metal Components using Additive Manufacturing**. American Welding Society, 2019.

ISSN 1983-1838

(DOI): 10.18624/etech.v17i1.1322

BAR-MEIR, G. **Fundamentals of Compressible Flow Mechanics**. Published by the author, 2007. Available at <https://potto.org/gasDynamics/node129.php> (Accessed on Oct. 12th, 2023).

BERGMAN, T. L.; LAVINE, A. S.; INCROPERA, F. P.; DeWITT, D. P. **Fundamentals of Heat and Mass Transfer**. 6th ed., Hoboken, NJ: Wiley, 2011. p. 10, 451, 571.

CUSHMAN-ROISIN, B. **Environmental Fluid Mechanic**. Published by the author, 2022. Available at <https://cushman.host.dartmouth.edu/books/EFM/chap9.pdf> (Accessed on Oct. 12th, 2023).

ÇENGEL, Y. A.; CIMBALA, J. M. **Fluid Mechanics**. 3rd ed., p. 670, 367, New York: McGraw-Hill, 2015.

FERREIRA, R.P.; VILARINHO, L.O.; SCOTTI, A. Development and implementation of a software for wire arc additive manufacturing preprocessing planning: trajectory planning and machine code generation. **Welding in the World**, vol. 66, p. 455–470, 2022. Available at <https://doi.org/10.1007/s40194-021-01233-w> (Accessed on Jan. 17th, 2024).

FUKUSHIMA, F. T. **Application of Compressed Air Cooling System In Additive Manufacture by Electric Arc** (in Portuguese). Graduation thesis in Mechatronic Engineering, IFSC, 2023.

GRONG, Ø. **Metallurgical Modelling of Welding**. 2nd ed. London: The Institute of Materials, 1997. p. 3, 27.

ISO. **ISO/ASTM 52900:2021(en) Additive manufacturing — General principles — Fundamentals and vocabulary**. International Organization for Standardization, 2021.

ISO. **ISO/TR 25901-4:2016(en) Welding and allied processes — Vocabulary — Part 4: Arc welding**. International Organization for Standardization, 2016.

KOZAMERNIK, N.; BRAČUN, D.; KLOBČAR, D. “WAAM system with interpass temperature control and forced cooling for near-net-shape printing of small metal components.” **The International Journal of Advanced Manufacturing Technology**, vol. 110, p. 1955–1968, 2020. Available at <https://link.springer.com/article/10.1007/s00170-020-05958-8> (Accessed on Aug. 14th, 2023).

ISSN 1983-1838

(DOI): 10.18624/etech.v17i1.1322

PRODUCTIVITY GAIN IN WIRE ARC ADDITIVE MANUFACTURING BROUGHT BY ROBOT-INTEGRATED COOLING SYSTEM USING COMPRESSED AIR

ERWIN TEICHMANN
LUCIANO AMAURY DOS SANTOS
FELIPE TABATA FUKUSHIMA
GUILLEN ETCHEMENDY
TEO BOUTILLIER
RAFAEL NUNES

LE, V. T.; MAI, D. S.; PARIS, H. Influences of the compressed dry air-based active cooling on external and internal qualities of wire-arc additive manufactured thin-walled SS308L components. **Journal of Manufacturing Processes**, vol. 62, p. 18-27, 2021. Available at <https://www.sciencedirect.com/science/article/pii/S1526612520308379> (Accessed on Sept. 12th, 2023).

MX3D. MetalXL: Design to print in one workflow software solution, 2024. Available at <https://mx3d.com/software/metalxl/> (Accessed on Feb. 11th, 2024).

NUNES, R.; VANDERMEIREN, N.; VERLINDE, W.; BORUAH, MOTTE, D. R.; De WAELE, W. A Benchmark of Mechanical Properties and Operational Parameters of Different Steel Filler Metals for Wire Arc Additive Manufacturing. **The International Journal of Advanced Manufacturing Technology**. vol. 127, p. 599–613, 2023. Available at <https://doi.org/10.1007/s00170-023-11520-z> (Accessed on Dec. 10th, 2023).

POPE, S. B. **Turbulent Flows**. Cambridge: Cambridge University Press, 2000. p. 96-134.

ROSENTHAL, D. Mathematical Theory of Heat Distribution During Welding and Cutting. **Welding Journal**, vol. 20, p. 220s-234s, 1941.

SANTOS, L. A.; SILVA, A. F. C. A Model for the Circumferential Welding of Tubes of Thin Wall (in Portuguese). *In*: **9th Brazilian Congress of Thermal Engineering and Science**, Rio de Janeiro: ABCM, Paper CIT02-0112, 2002. Available at <https://abcm.org.br/app/webroot/anais/encit/2002/Paper-title/32/CIT02-0112.pdf> (Accessed on Oct. 12th, 2023).

SHAPIRO, A. H. **Dynamics and Thermodynamics of Compressible Fluid Flow**. Volume 1, New York: The Ronald Press Company, 1953. p. 178-185.

SPRUTCAM. SprutCAM X Robot: innovative all-in-one CAD/CAM/OLP for robots, 2024. Available at < https://sprutcam.com/sprutcam-x-robot/> (Accessed on Feb. 11th, 2024).

TEICHMANN, E. W.; PAMPLONA, G. R.; DUTRA, C. B. S.; RODRIGUES, M. B. **Cooling System for Additive Manufacture** (in Portuguese). Brazilian Patent Number BR1020190057050, Brazil: INPI, 2019.

ISSN 1983-1838

(DOI): 10.18624/etech.v17i1.1322

eTECH
TECNOLOGIAS PARA
COMPETITIVIDADE INDUSTRIAL

PRODUCTIVITY GAIN IN WIRE ARC ADDITIVE MANUFACTURING BROUGHT BY ROBOT-INTEGRATED COOLING SYSTEM USING COMPRESSED AIR

ERWIN TEICHMANN
LUCIANO AMAURY DOS SANTOS
FELIPE TABATA FUKUSHIMA
GUILLEN ETCHEMENDY
TEO BOUTILLIER
RAFAEL NUNES

VERLINDE, W.; NUNES, R.; RYMENANT, P. V.; CHERNOVOL, N.; ANTHONE, T. **Practical Guideline – 3D Printing with Gas Metal Arc Welding**. Belgium Institute of Welding, 2021. Available at < https://bil-ibs.be/en/node/2213> (Accessed on Jan. 16th, 2024).

WU, B.; DING, D.; PAN, Z; CUIURI, D.; LI, H.; HAN, J.; FEI, Z. Effects of heat accumulation on the arc characteristics and metal transfer behavior in Wire Arc Additive Manufacturing of Ti6Al4V. **Journal of Materials Processing Technology**, vol. 250, p. 304-312, 2017. Available at <https://www.sciencedirect.com/science/article/pii/S0924013617303370> (Accessed on Oct. 12th, 2023).